Journal of Neural Engineering

PAPER

Fractional-order model predictive control as a framework for electrical neurostimulation in epilepsy

Sarthak Chatterjee[1], Orlando Romero[2], Arian Ashourvan[3] and Sérgio Pequito[2]

[1] Department of Electrical, Computer, and Systems Engineering, Rensselaer Polytechnic Institute, Troy, NY 12180 United States of America
[2] Department of Industrial and Systems Engineering, Rensselaer Polytechnic Institute, Troy, NY 12180 United States of America
[3] Penn Center for Neuroengineering and Therapeutics, University of Pennsylvania, Philadelphia, PA 19104 United States of America

E-mail: chatts3@rpi.edu

RECEIVED
20 May 2020

REVISED
19 September 2020

ACCEPTED FOR PUBLICATION
3 November 2020

PUBLISHED
16 December 2020

Keywords: fractional-order dynamical systems, epileptic seizure mitigation, model predictive control, electrical neurostimulation

Supplementary material for this article is available online

Abstract

Objective. Electrical neurostimulation is an increasingly adopted therapeutic methodology for neurological conditions such as epilepsy. Electrical neurostimulation devices are commonly characterized by their limited sensing, actuating, and computational capabilities. However, the sensing mechanisms are often used only for their detection potential (e.g. to detect seizures), which automatically and dynamically trigger the actuation capabilities, but ultimately deploy prespecified stimulation doses that resulted from a period of manual (and empirical) calibration. The potential information contained in the measurements acquired by the sensing mechanisms is, therefore, considerably underutilized, given that this type of stimulation strategy only entails an event-triggered relationship between the sensors and actuators of the device. Such stimulation strategies are suboptimal in general and lack theoretical guarantees regarding their performance. *Approach.* In order to leverage the aforementioned information, harvested during normal sensing-actuating operation, we must consider a real-time feedback (*closed-loop*) strategy. More precisely, the stimulation signal itself should automatically adapt based upon the state of the neurophysiological system at hand, estimated from data collected in real-time through sensors in the device. *Main results.* In this work, we propose a model-based approach for (real-time) closed-loop electrical neurostimulation, in which the evolution of the system is captured by a fractional-order system (FOS). More precisely, we propose a *model predictive control* (MPC) approach with an underlying FOS predictive model, due to the ability of fractional-order dynamics to more accurately capture the long-term dependence present in biological systems, compared to the standard linear time-invariant models. Furthermore, MPC offers, by design, an additional layer of robustness to compensate for system-model mismatch, which the more traditional strategies lack. To establish the potential of our framework, we focus on epileptic seizure mitigation by computational simulation of our proposed strategy upon seizure-like events. Lastly, we provide evidence of the effectiveness of our method on seizures simulated by commonly adopted models in the neuroscience and medical community present in the literature, as well as real seizure data as obtained from subjects with epilepsy. *Significance* Our study thus paves the way for the development and implementation of robust real-time closed-loop electrical neurostimulation which can then be used for the construction of more effective devices for epileptic seizure mitigation.

1. Introduction

Electrical neurostimulation refers to the activation or modulation of part of the nervous system for the mitigation of neurological disorders. Although neurostimulation has become an important therapeutic method associated with disorders of the central or peripheral nervous systems, we are still in the early days of understanding the delicate balance between the sensing, actuation, and computational capabilities of electrical neurostimulation devices. Many of these aforementioned devices use pre-determined actuation strategies which leaves a lot of scope for the development of real-time actuation strategies that accommodate for changes in the data captured by the sensors.

In healthcare applications, electrical neurostimulation brings the promise of enabling continuous interaction with patients, toward ensuring or enhancing the individual's quality of life. As a consequence, electrical neurostimulation possesses the potential to lower healthcare costs for prevention and therapies associated with chronic diseases (e.g. neurological disorders and diseases such as epilepsy, Alzheimer's, and Parkinson's). To fulfill its promise, a coherent model-based theory should be devised, allowing us to capture the spatiotemporal nature of human physiological processes. By doing so, personalized neurostimulation schemes (i.e. specific to the individual's physiology) can be implemented to perform continuous monitoring and risk assessment of abnormal behavior that will enable a real-time response from the controlling device (e.g. an electrical neurostimulator).

In the context of neurophysiological signals, *temporal* fractional properties in both health and disease states have become apparent and with a huge potential for clinical applications [1–7]. Geometrically, such properties entail self-similarity of signals at different time scales. Practically, this leads signals to become non-stationary and to possess long-term memory dependencies with themselves, with the backward-decaying weights of such dependencies following a power-law distribution [8]. Nonetheless, only recently have dynamical *spatiotemporal* fractional models been proposed as a tool to model neurophysiological signals suitable to deal with structured data and to equip us with modeling capabilities that capture spatial (i.e. the contributions of the signal's components into each other) and temporal long-range memory through the so-called fractional-order coefficients associated with the power-law exponents [9–15], and possibly under unknown unknowns [16, 17].

Notwithstanding the above, the main advent of model-based approaches is that we can understand how an external signal or stimulus would craft the dynamics of the process. Simply speaking, it enables us to *design* a sequence of interactions (i.e. a control strategy or law) with the system such that we can steer its dynamics toward satisfying desirable properties. That said, due to the highly dynamical nature of the neurophysiological processes, it is imperative that we consider *feedback* mechanisms [18]. In other words, we need to leverage the continuous flow of measurements of the system to tune (for the individual's process) the control strategy. A particularly successful strategy that has achieved remarkable success in several engineering applications is the strategy of *model predictive control* (MPC) that consists of three key ideas [19–24]: (*i*) a model-based approach; (*ii*) capability of predicting the evolution of the system and its states upon a devised feedback control strategy that aims to optimize an objective that encapsulates the risk assessment of abnormal behavior; and (*iii*) receding finite-horizon re-evaluation of the control strategy performance devised in the previous point.

In the context of neurophysiological processes, we propose to leverage fractional-order models to equip us with the aforementioned prediction and control capabilities that go hand in hand with the closed-loop design of neurostimulators. As a consequence, we will be able to develop stimulation strategies that will minimize the overall duration and/or strength of seizures (i.e. we aim to mitigate their effect). Notwithstanding, we believe that similar design and strategies can be envisioned in other contexts where closed-loop deep-brain electrical stimulation is available—Parkinson's [25, 26], Alzheimer's [27], depression [28, 29], and anxiety [30], just to mention a few.

To summarize, in what follows we introduce in a pedagogical manner the control mechanisms to be deployed as part of future neurophysiological cyber-physical systems, with particular emphasis on electrical neurostimulation for epilepsy. Ultimately, the integration of these design features will lead to more reliable neurostimulators that will immediately improve, or otherwise bring a positive impact, on the quality of life of the patients that qualify for the use of such technologies.

2. Data and methods

2.1. Epilepsy and neurostimulation

Epilepsy is a neurological disorder that, according to the Michigan Epilepsy Foundation, affects roughly 1% of the American population (with similar rates worldwide). Nearly 4% of Americans will develop some form of epilepsy during their lives, and it is the fourth most common neurological disorder in the United States after migraine, stroke, and Alzheimer's disease [31, 32]. Epilepsy is characterized by a predisposition to *(epileptic) seizures* and their associated consequences. Seizures are often associated with episodes of abnormal, excessive, and/or highly synchronized brain activity, which often result in a temporary

disturbance in brain function (e.g. motor, sensory, and mental faculties) [33].

To monitor seizures, we can use standard brainwave monitoring technologies such as the electroencephalogram (EEG) and intracranial electroencephalogram (iEEG). Both of these monitoring technologies have their foundations on the similar principle of using electrodes to measure electric potential differences (voltages) that roughly translate to local brain activity. More precisely, in EEG, the electrodes are placed in direct contact with the scalp of the patient, whereas for iEEG, the electrodes are typically distributed among a thin rectangular grid, which is then placed in direct contact with neural tissue at the top of the brain through a surgical procedure. For instance, in figure 1, we can observe the start of a seizure-like period of activity using iEEG at around time $t = 20$ s. The period shortly before a seizure is often referred to as a *pre-ictal* period. These readings can also be analyzed in several other ways, both by visual inspection and by more quantitative methods [34].

2.2. Categories of seizures and epilepsy

Seizures can be categorized in several ways, one of which is concerned with whether the seizure originates from an isolated region on a single hemisphere of the brain (this is known as a *partial*, *focal onset*, or *localized* seizure), or if they affect both hemispheres from the start (this is known as a *generalized* or *multifocal* seizure). The region of origin of a seizure is called the *epileptogenic zone*, and the period for which it lasts is referred to as the *onset*. There are further categories and subcategories for seizures and for epilepsy (based on the nature of the seizures), depending on whether or not the seizures include impaired awareness or motor function, convulsions, loss of consciousness, muscle jerks or stiffness, among others—see more details in [35].

2.3. Treatment of epilepsy

Several treatment options are available for epilepsy, whose success depends upon several factors such as age and type of seizures/epilepsy. For instance, a large portion of patients who suffer from convulsive seizures are successfully treated through anticonvulsant medication [36]. Many other patients report similar success for various other anti-seizure medications. For patients who do not respond well to medication or whose seizures are otherwise difficult to treat (associated with *refractory* epilepsy), we face a so-called *critical*, *intractable*, or *resistant* form of epilepsy, which is currently treated by either *resection* (i.e. surgical extraction) or electrical stimulation of the brain. The latter is known as *(electrical) neurostimulation*, and consists of the administration of small doses of currents applied, for example, to the vagus nerve [37, 38], the cortex [39], or the anterior nucleus of the thalamus [40, 41]. Additionally, stimulation may also be applied deeper into the brain in specific regions, which is commonly referred to as *deep brain stimulation* (DBS) [42]. In particular, for patients who suffer from focal epilepsy with a known seizure focus or epileptogenic zone, then, most commonly, the electrical stimulation is applied directly over these regions [43].

2.4. Electrical neurostimulation

Different strategies exist for electrical neurostimulation, which include *open-loop* and *closed-loop* strategies (also known as *brain-responsive* neurostimulation) that are carried out by an implementable device referred to as a *neurostimulator*. The neurostimulators are supplied with intracranial electrodes to measure brain activity and deliver current storage through an array of capacitors corresponding to the electrical stimuli.

Open-loop neurostimulation consists of any neurostimulation strategy that does not utilize current brain activity data to regulate the stimuli applied to the patient's brain. For instance, continuous DBS is a standard open-loop neurostimulation treatment option for Parkinson's disease [44], in which the electrical stimulation is continuously applied through a surgically implanted device, either during prespecified periods of the day (such as in the morning or at night) or throughout the entire day.

On the other hand, closed-loop (brain-responsive) neurostimulation consists of neurostimulation treatments based on automatic electrical stimulation directly influenced by the present (real-time) behavior being observed through continuous recording of brain activity. Past data can also be used in this strategy, but due to limited storage memory, these neurostimulation mechanisms are usually designed to depend exclusively on the actual recorded and stored data at a given time, consisting of a finite temporal window ranging from a fixed number of past instances of discretized time to the present measurement.

2.5. Neurostimulator for epilepsy

Currently, in the USA, examples of the U.S. Food and Drug Administration approved neurostimulators for epilepsy (i.e. to mitigate seizures) are the RNS® (responsive neuro stimulation) system [45] (developed by the company NeuroPace®) and Medtronic's DBS system. The former differs from the latter in that it is a brain-responsive (as compared to open-loop) strategy. The RNS® device manufactured by NeuroPace® consists of a battery pack and a small processor, a lead strip containing four connected electrodes, and either an additional strip or a lead tube that is inserted deep into the brain. In the first case, the two strips are typically placed symmetrically to the localized seizure focus. For the second configuration, the single strip is placed directly on the seizure focus. For the purpose of this work, we will exclusively focus on the single-strip configuration.

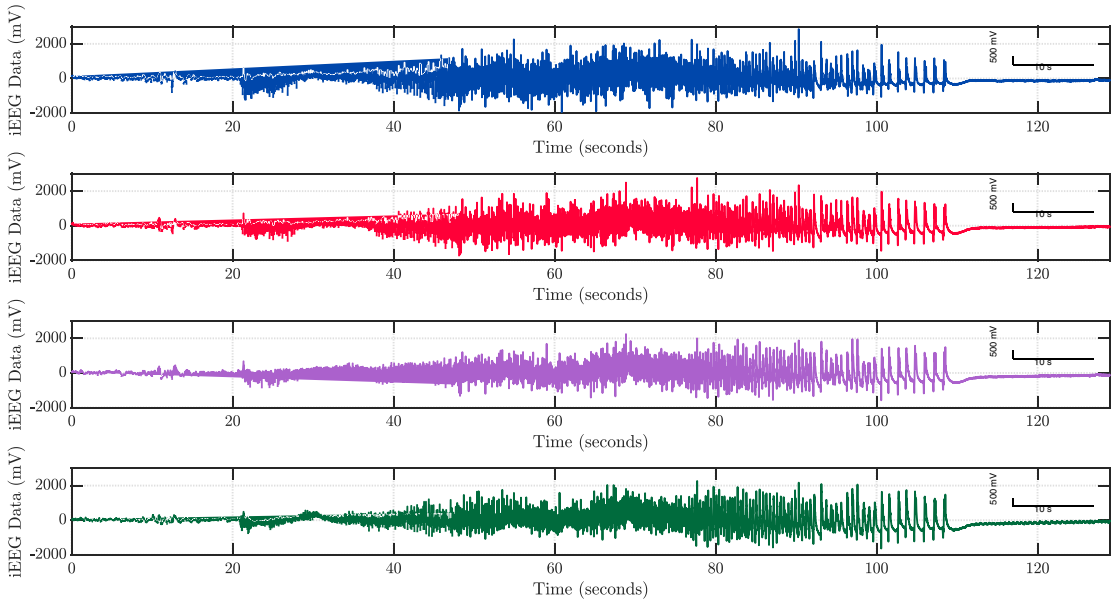

Figure 1. Multivariate 4-channel iEEG signal depicting the start of a seizure in a subject suffering from epilepsy. The clinical seizure onset is 20 s into the iEEG segment and the offset is 20 s before the end of the sample. This data was collected from a subject undergoing a secondary generalized seizure.

The RNS® is programmed with algorithms that attempt to detect when a seizure is in progress—see the recent survey on detection methods in [46]. As soon as a seizure is detected, the device will stimulate the brain at the location of one (or more) of the intracranial electrodes by generating a biphasic voltage pulse through an integrated voltage generator circuit, which, in turn, translates to small stimulating currents. The voltage generator contains programmable waveform (e.g. rectangular and sinusoidal), amplitude, frequency, phase, and duration [39, 47]. Despite the closed-loop nature of the RNS® system, the various parameters that characterize the stimulation signal are (currently) not dynamically adapted to reflect an optimal control strategy based on the data that is currently being measured.

2.6. Fundamentals of state space and feedback control theory

In dynamical systems theory [48, 49], *state-space models* describe the evolution over time of dynamical systems through a finite set of time-dependent variables (or *signals*) $x_1(t), \ldots, x_n(t) \in \mathbb{R}$ called *state variables*, or (collectively) the *state vector* $x(t) \in \mathbb{R}^n$. The state vector is usually understood as a minimal collection of variables that contains a sufficient statistic of the system (i.e. the entire future of the system can be fully predicted, apart from possible noise signals). Simply speaking, knowledge of $x(t_0)$ and the model suffices to fully predict $x(t)$ for every $t \geq t_0$.

For the purposes of this paper, the first N components of $x(t)$ may correspond to the measurements from an N-channel iEEG sensing technology. For instance, for the standard configurations of the RNS® system with two intracranial electrode strips, we will have $N = 4$ channels. Notwithstanding, we may have $n \geq N$ state variables, with the remaining $n - N$ state variables representing hidden or latent signals that influence, directly or indirectly, the evolution of measured signals and thus, the underlying system itself.

While state variables are usually described as temporal signals in the majority of the literature, in certain areas, they may also be spatio-temporal. The spatial component may be included as either additional independent variables of the state variables or by a mapping of some subset of the state variables to spatial locations such as in the iEEG case, in which each state variable corresponds to the concrete physical location of its corresponding electrode [50].

The evolution of a neurophysiological system is often modeled through a system of first-order ordinary difference equations

$$x_{k+1} = f(k, x_k) \tag{1}$$

for $k \in \mathbb{Z}_+$, where $f : \mathbb{Z}_+ \times \mathbb{R}^n \to \mathbb{R}^n$ is a known function. However, identifying and mathematically modeling the respective relationships between all the hidden signals that relate to the actually measured brain signals is currently a fundamentally intractable task. For this reason, we will adopt the common perspective in which the state variables will be exclusively constituted by the N measurable brain signals (one for each channel), and the influence of external signals will be modeled as additive noise, which can be described by

$$x_{k+1} = f(k, x_k) + w_k \tag{2}$$

for $k \in \mathbb{Z}_+$. It is important to notice that, whether the noise signal w_k is modeled as a random vector or just an unknown deterministic signal, the initial state is insufficient to make an accurate prediction of the evolution of the system due to the unknown disturbance. In this paper, as in many other applications, we will model w_k as additive white Gaussian noise (AWGN).

A core problem in state-space control theory [51] is that of determining how (or if it is even possible) to steer the state of a system from its initial state $x_{\text{init}} \in \mathbb{R}^n$ toward a particular desired state $x_{\text{des}} \in \mathbb{R}^n$ through a finite number of manipulated *input signals* administered on the system. In the context of the present work, the input corresponds to an exogenous electrical stimulus [52, 53]. Specifically, we focus on the electrical stimulation scenario for epileptic seizure mitigation, where the control objective is to steer the state of the neurophysiological system (i.e. its iEEG recordings) away from a period of seizure-like activity.

The vector input signal (which lumps together all input signals at a specific time) is denoted by $u_k \in \mathbb{R}^{n_u}$ for $k \in \mathbb{Z}_+$. If the choice of the input signal has the potential to perturb the dynamics of the system, then our state-space model now becomes of the form

$$x_{k+1} = f(k, x_k, u_k), \tag{3}$$

where now $f : \mathbb{Z}_+ \times \mathbb{R}^n \times \mathbb{R}^{n_u} \to \mathbb{R}^n$. Therefore, the evolution of the system is fully determined by the state vector, and now the control input being applied. As a consequence, every measurement we take on the system (obtained through the use of sensors) can be typically modeled as a function of the current state and input. For instance, in our working electrically stimulated neurophysiological system, we may utilize each electrode as both a sensor and an actuator because they are designed for convenient conductance of electric charges. However, each electrode may not be used simultaneously as both a sensor and an actuator for reasons of interference.

Mathematically, we may consider each electrode as a sensor whose measurements can be written as $y_{i,k} = h_i(x_{i,k}, u_{i,k})$ such that $h_i(x, 0) = h_{i,\text{const}}$ and $h_i(x, u) = u$ for $y \neq 0$, where $x_{i,k}$ and $u_{i,k}$ denote, respectively, the ith electrode's theoretical reading and voltage input. In other words, if no stimulation is being applied at time step $k = K$ (i.e. $u_{i,K} = 0$), then the measured value will be $y_{i,K} = h_i(x_{i,K}, 0) = h_{i,\text{const}}$. On the other hand, if an electrical stimulus is being applied (i.e. $u_{i,K} \neq 0$), then the measurement is uninformative of the state of the system (i.e. $y_{i,K} = h_i(x_{i,K}, u_{i,K}) = u_{i,K}$). Alternatively, we may consider a model such as $y_{i,k} = h_i(x_{i,k}, u_{i,k}, w_{i,k})$, with $h_i(x, u, w) = x + uw$ and $w_{i,k}$ denotes a stationary white process, so that $x_{i,K}$ can be precisely retrieved from $y_{i,K}$ if $u_{i,K} = 0$, whereas it can only be estimated with deteriorating estimation quality as $u_{i,K}$ increases. From a physical perspective, this situation boils down to modeling the interference of the electrical simulation as increased noise on the attempted measurement of the theoretical electrode's reading.

In state-space systems theory, we typically assume our measurements to be temporal signals lumped together as a vector *output signal*, which will be denoted as y_k when working in discrete time. In particular, they are often modeled, in general, as

$$y_k = h(k, x_k, u_k), \tag{4}$$

where $h : \mathbb{T}_+ \times \mathbb{R}^n \times \mathbb{R}^{n_u} \to \mathbb{R}^{n_y}$ is a known function. Such measurements may be used for a variety of tasks, most importantly of which includes *state estimation* [51]. When conducted in real-time, state estimators may be used to regulate the input signal in order to achieve the desired control. This occurs since, naturally, the underlying known input–output relationship (possibly affected by noise) is known, and the measurements typically contain partial information regarding the current state of the system, since the initial state may be unknown, or process noise may be present. Furthermore, there could also be a mismatch between the real system and its mathematical model, which may lead to poor control laws, when these are designed in open-loop. In other words, designed without providing the controller access to any output signal.

State-space systems constructed in the fashion described above, where the control input is automatically and explicitly determined based on the measured signals (i.e. the output signal), are referred to as *closed-loop* (or *feedback*) systems. In other words, $u_k = g(k, y_k)$ for discrete-time systems. Furthermore, the *optimal* control law (i.e. the stimulation strategy) should be determined toward satisfying a specified goal that is encoded as part of an optimization problem. For the purposes of this paper, the control objective will be to steer measured brain signals during an ictal period toward a normal range of activity through electrical stimulation. As such, the optimization problem will encode and penalize the difference with respect to the goal, as well as account for the total use of the actuation (i.e. electrical stimulation).

2.7. Fractional-order systems

For many biological systems, the state-space models discussed so far are insufficient to accurately capture the real evolution of the systems for anything other than a very small interval of time into the future, given that the current state of the system may have a non-negligible dependence on several past states, or even from the states ranging from the entire period of time so far. For these reasons, we introduce the so-called (linear) *fractional-order system* (FOS) models, described as follows:

$$\Delta^{\alpha} x_{k+1} = Ax_k + Bu_k + w_k, \tag{5}$$

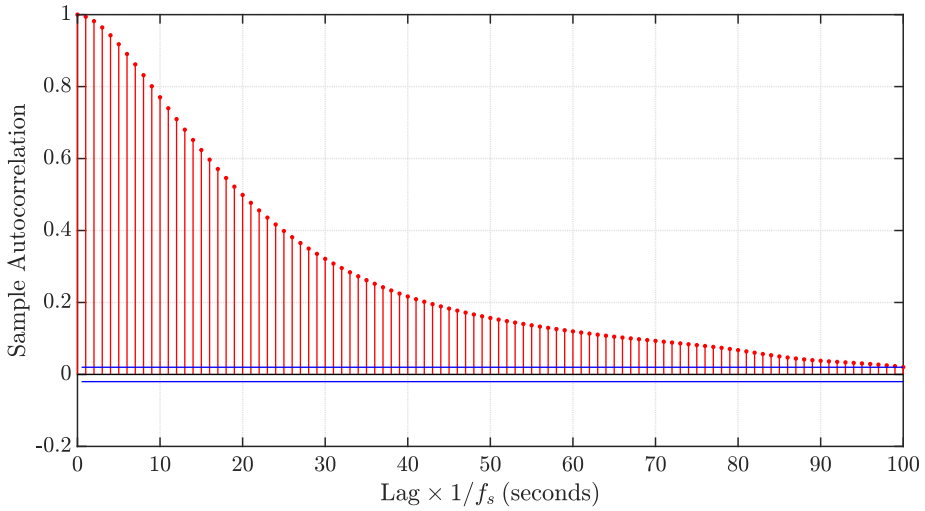

Figure 2. Sample autocorrelation function profile of a seizure simulated by the Jansen–Rit neural mass model [61]. The slow non-exponential decay with non-negligible values even at long lags are characteristic of processes having intrinsic long-term memory. The lag is represented as multiples of the reciprocal of the sampling frequency f_s, with $f_s = 1000$ Hz.

where $A \in \mathbb{R}^{n\times n}$ is the *state coupling matrix* and $\alpha \in \mathbb{R}^n_+$ is the vector of *fractional-order* coefficients. Simply put, larger values of the fractional-order coefficients imply a lower dependency on the previous data from that state (i.e. a faster decay of the weights used as linear combination of previous data). The signal $u_k \in \mathbb{R}^{n_u}$ denotes the *input* corresponding to the *actuation signal* and the matrix $B \in \mathbb{R}^{n\times n_u}$ is the *input matrix* that scales the actuation signal. The term w_k denotes a sequence of independent random vectors, each following a normal distribution $\mathcal{N}(0,\Sigma)$ with the covariance matrix $\Sigma \in \mathbb{R}^{n\times n}$. These models are similar to classical discrete-time linear time-invariant system models with the exception of the inclusion of the fractional derivative, whose expansion and discretization for the ith state, $1 \leq i \leq n$, can be expressed as

$$\Delta^{\alpha_i} x_{i,k} = \sum_{j=0}^{k} \psi(\alpha_i, j) x_{i,k-j}, \tag{6}$$

where α_i is the fractional-order coefficient corresponding to the state i and

$$\psi(\alpha_i, j) = \frac{\Gamma(j-\alpha_i)}{\Gamma(-\alpha_i)\Gamma(j+1)}, \tag{7}$$

with $\Gamma(\cdot)$ being the gamma function defined by $\Gamma(z) = \int_0^\infty s^{z-1}e^{-s}\,\mathrm{d}s$ for all complex numbers z with $\Re(z) > 0$ [18] – see Supplementary Material (https://stacks.iop.org/JNE/17/066017/mmedia) for more details.

FOSs have found use in modeling complex spatiotemporal dynamics interacting across varying time scales in both space and time. Mechanisms where there is a sudden and critical shift in dynamics have been widely documented in the literature from multiple points of view [54, 55]. The work in [56] provides evidence that multiple time scale adaptations in rat neocortical pyramidal neurons can be explained using fractional differentiation phenomena. Furthermore, in the domain of epileptic seizures, we are aware of works that attempt to classify [57] and predict [58] seizures using FOS theory.

A further convincing argument behind the use of fractional-order models can be made as follows. The non-negligible dependence of the current state of the system on several past states can be well understood from the sample autocorrelation functions (sACFs) of the time series data that simulate an epileptic seizure. We consider the sACFs of the time series seizure data simulated by the models considered in this paper as well as the data presented in figure 1. From figures 2–5, we find that the said autocorrelation functions demonstrate that their decay is algebraic and slower than exponential such that the area enclosed by the composite autocorrelation function curve is infinite. Such slowly decaying autocorrelation functions with non-negligible values even at long lags are typical of processes having intrinsic long-range memory and are modeled well with fractional derivatives [59, 60].

2.8. Fractional-order MPC

MPC is a control strategy that allows the control of processes while satisfying a set of constraints. Having its origins in the chemical process industry in the 1980s, MPC has been successfully used in fields such as automotive engineering, aerospace, and the food and beverage processing industry, to just mention a few. At its core, MPC uses explicit process models (which may be linear or non-linear) to predict how a plant will respond to arbitrary inputs. For each instant of time, an MPC algorithm seeks to optimize plant behavior in the future by computing a series of control inputs over a time horizon called the *prediction horizon* by solving an optimization problem—often with constraints. Once this step is

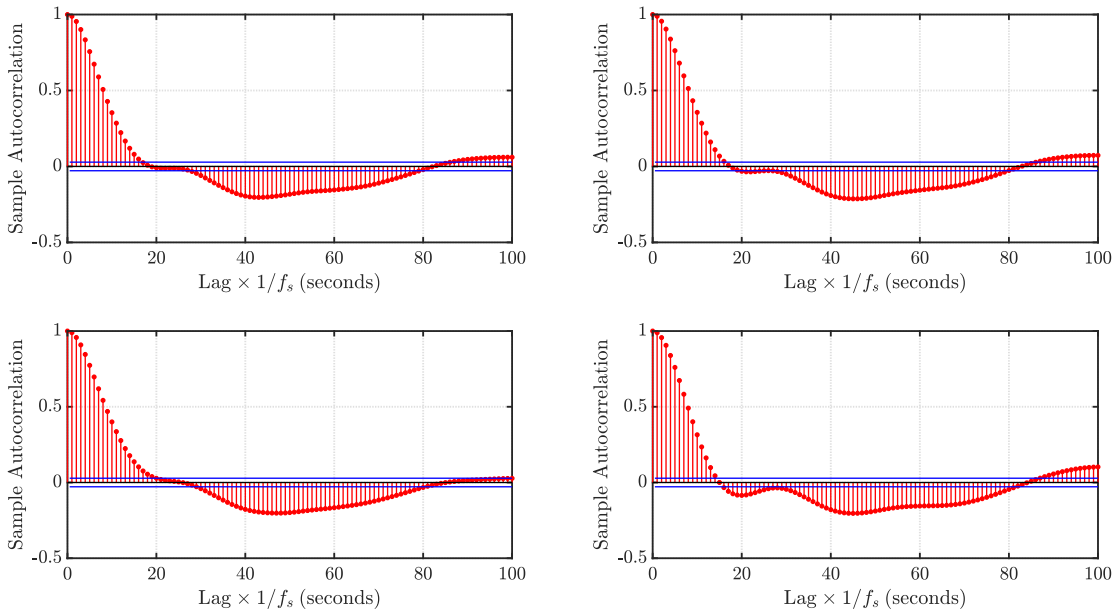

Figure 3. Sample autocorrelation function profile of a seizure simulated by the model described in Martinet *et al* [62]. The lag is represented as multiples of the reciprocal of the sampling frequency f_s, with $f_s = 500$ Hz.

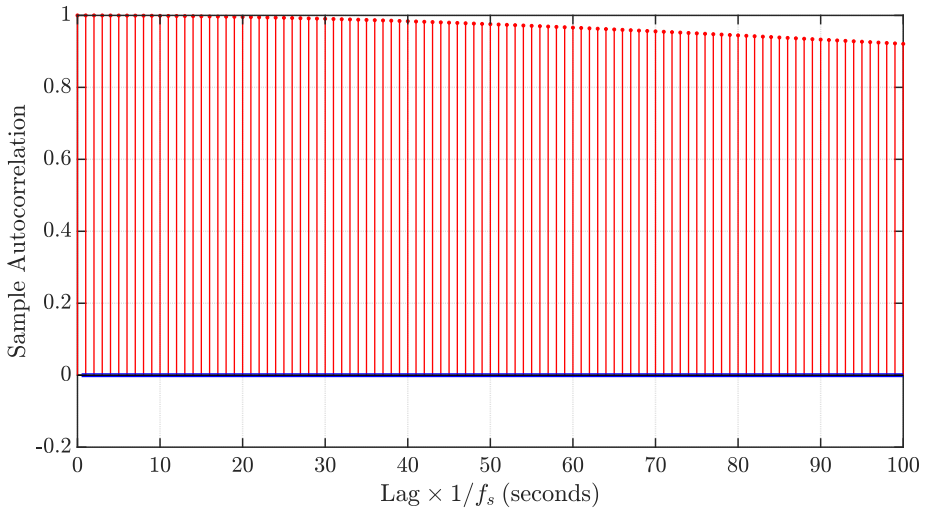

Figure 4. Sample autocorrelation function profile of a seizure simulated by the Epileptor model described in Jirsa *et al* [63]. The lag is represented as multiples of the reciprocal of the sampling frequency f_s, with $f_s = 1000$ Hz.

complete, the computed control inputs corresponding to the first subsection of the prediction horizon (called the *control horizon*) are then sent to the plant. This procedure is then repeated at subsequent control intervals [21]. This receding horizon strategy implicitly introduces *closed-loop feedback*.

Subsequently, in this section, we propose a (state-space) model-based approach where the predictive model is obtained from a linear FOS. Based on the state signal's evolution predicted by the model, and by regarding the impact of an arbitrary control input signal in the state's evolution, we can set out to adapt the stimulation signal in real-time by choosing the parameters that lead to stimulation signals within a safe range toward optimizing some measure of performance that encapsulates the goal of steering abnormal activity to normal ranges. In general, however, our predictive model will not precisely match the real dynamics of the system. Therefore, our proposed stimulation strategy will periodically re-evaluate the current estimated state and corresponding predictions, and re-compute the appropriate optimal stimulation strategy. MPC is equipped with all the features mentioned above and tends to be considerably more robust [64, 65] than other (more classical) strategies like using fractional-order proportional-integral-derivative controllers, a modification of a classical technique used in feedback control theory, to suppress seizures simulated using a linearized neural mass model [66].

In the fractional-order MPC framework which we will use, we will focus on the design of a

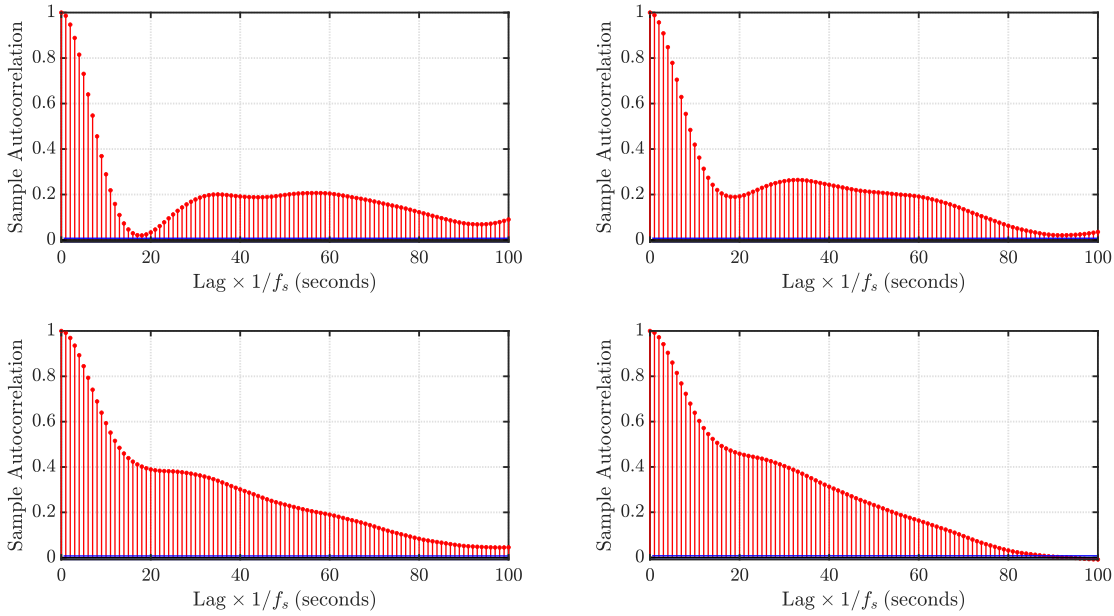

Figure 5. Sample autocorrelation function profile of the real seizure data presented in figure 1. The lag is represented as multiples of the reciprocal of the sampling frequency f_s, with $f_s = 512$ Hz.

model predictive controller for a (possibly time-varying) discrete-time fractional-order dynamical system model

$$\Delta^{\alpha} x_{k+1} = A_k x_k + B_k u_k + B_k^w w_k, \tag{8}$$

where w_k denotes a sequence of independent and identically distributed random vectors, following an $\mathcal{N}(0, \Sigma)$ distribution (with the covariance matrix $\Sigma \in \mathbb{R}^{n\times n}$) and B_k^w denotes the matrix of weights that scales the noise term w_k. The objective is to design the feedback controller such that it minimizes a quadratic cost functional of the input and state vectors over a finite time horizon P (the prediction horizon). In other words, the objective is to determine the sequence of control inputs $u_k, \ldots, u_{k+P-1}$ that minimizes a quadratic cost function of the form

$$\begin{aligned} &\text{(cost function)} \quad \underset{u_k,\ldots,u_{k+P-1}}{\text{minimize}} \quad \mathbb{E}\left\{ \sum_{j=1}^{P} \|x_{k+j}\|^2_{Q_{k+j}} + \sum_{j=1}^{P} c_{k+j}^{\mathsf{T}} x_{k+j} + \sum_{j=0}^{P-1} \|u_{k+j}\|^2_{R_{k+j}} \right\} \\ &\text{(constraints)} \quad \text{subject to} \quad x_k = \text{observed or estimated current state} \\ &\qquad\qquad \Delta^{\alpha} x_{k+j+1} = A_{k+j} x_{k+j} + B_{k+j} u_{k+j} + B^w_{k+j} w_{k+j}, \quad j = 0, 1, \ldots, P-1, \\ &\qquad\qquad \text{other linear constraints on } x_{k+1}, \ldots, x_{k+P}, u_k, \ldots, u_{k+P-1}, \end{aligned} \tag{9}$$

where $Q_{k+1}, \ldots, Q_{k+P} \in \mathbb{R}^{n\times n}$ and $R_k, \ldots, R_{k+P-1} \in \mathbb{R}^{n_u \times n_u}$ are given positive semidefinite matrices. Here, $Q \in \mathbb{R}^{n\times n}$ is a *positive semidefinite* matrix if $x^{\mathsf{T}} Q x \geq 0$ for every $x \in \mathbb{R}^n$, and $\|x\|_Q = \sqrt{x^{\mathsf{T}} Q x}$ in that case. For seizure mitigation via electrical neurostimulation, we propose to use $Q_j = I_{n\times n}$, $c_j = 0_{n\times 1}$, and $R_j = \varepsilon I_{n_u \times n_u}$ with $\varepsilon > 0$ for all j, such that the objective becomes largely to steer the total energy in the expected value of the brain signals toward the smallest amount possible—see Supplementary Material for further details.

The quadratic term on the input, which represents the electrical neurostimulation signal, is intended to add a penalization term for stimulating the patient too harshly, since this may be unsafe, create discomfort for the patient, or result in harmful psychological effects [67]. It is also interesting to note that even if we need the estimation of the system states in the above problem, the presence of a separation principle for discrete-time fractional-order systems [68] gives us guarantees that we can perform MPC with state estimation for these systems.

Note that, here, P is called the *prediction horizon*, and the framework only deploys the control strategy associated with the first M time steps (referred to as the *control horizon*). Simply speaking, after we reach state x_{k+M-1}, we update k with $k+M-1$ and recompute the new solution. This way, we have

robust solutions, since, by design, the optimal strategy is constantly being re-evaluated based on the short-term control action implementation of a long-term prediction [69].

3. Simulation results

In what follows, we propose to illustrate the use of the fractional-order MPC framework for neurostimulation in the context of mitigating epileptic seizures. We demonstrate the workings of the proposed approach on four different experimental scenarios relying primarily on iEEG data: *(i)* an iEEG signal demonstrating an epileptic seizure simulated by the neural mass model proposed by Jansen and Rit [61, 70]; *(ii)* an iEEG signal simulated by a neural field model proposed in [62] that replicates the spatiotemporal dynamics of a seizure; *(iii)* an iEEG signal simulated by the phenomenological 'Epileptor' model proposed in [63]; and *(iv)* real-time iEEG signals for three human subjects undergoing epileptic seizures. For all of the above cases, we start by considering an epileptic seizure captured by a linear FOS model whose parameters are obtained through a system identification method using brainwave data obtained from iEEGs.

3.1. Epileptic seizure simulated by the Jansen–Rit neural mass model

3.1.1. Brief description of the model

Although initially proposed to account for human EEG rhythms and visual evoked potentials, the Jansen–Rit neural mass model has also been used to shed light on human epileptiform brain dynamics [71, 72]. The Jansen–Rit neural mass model is composed of three interacting subpopulations which include the main subpopulation, the excitatory feedback subpopulation, and the inhibitory feedback subpopulation. The structure of the model is such that the main subpopulation comprises cells that receive neuronal signals in feedback from the excitatory and inhibitory subpopulations (see Supplementary Material for a detailed description of the model and the standard parameter values used).

The use of neural mass models akin to the Jansen–Rit model in feedback control frameworks is well documented. The works in [66, 73–77] all use neural mass models from the point of view of control theory for the suppression of epileptic seizures. In what follows, we will demonstrate the effectiveness of our proposed control strategy on a seizure simulated by the classical Jansen–Rit neural mass model with standard parameter values—see Supplementary Material.

3.1.2. System identification through parameter estimation on seizures simulated by the Jansen–Rit neural mass model

First, we need to determine the parameters A and α that model both spatial coupling and fractional coefficients, respectively, that craft the evolution of the state $x_k \in \mathbb{R}^n$ in the FOS model

$$\Delta^{\alpha} x_{k+1} = Ax_k + Bu_k + B^w w_k, \tag{10}$$

with w_k denoting AWGN. Since the system is single-input-single-output (SISO), we have both A and α to be scalars. To identify the parameters A and α, we used the method proposed in [16]. The parameters obtained are $A = -0.0054$ and $\alpha = 1.4881$. Furthermore, we assume that $B = 1$ and $B^w = 0.1$.

3.1.3. Closed-loop electrical neurostimulation using FOS-MPC

For the cost function in (9), we utilized $Q_k = I_n$, $R_k = I_{n_u}$, and $c_k = 0_{n_u \times 1}$ (with $n = n_u = 1$), to emphasize minimizing the overall energy in the measured iEEG signal, while penalizing slightly for overly aggressive stimulation. Furthermore, we included a safety linear constraint of $-5 \leq u_k \leq 5$. Our predictive model was based on a $(p = 15)$–step (15 ms) predictive model approximation of the FOS plant (see Supplementary Material), with a $(P = 20)$–step (20 ms) prediction horizon and $(M = 10)$–step (10 ms) control horizon. The results are presented in figure 6, which provide evidence that the proposed stimulation strategy allows us to achieve amplitude suppression using a (time-varying) impulse-like stimulation scheme. Note that the actuation signal u_k kicks in at about the 4 s mark in the figure.

3.2. Epileptic seizure simulated by the mean-field model proposed by Martinet *et al* [62]

Next, we turn our attention toward a computational model that uses traveling wave dynamics to capture inter-scale coupling phenomena between large-scale neural populations in the cortex and small-scale groups in cortical columns [62]. Modeling the complex spatiotemporal dynamics of epileptic seizures is a challenging task, primarily because of the interaction of myriad scales in both time and space.

3.2.1. Brief description of the model

The neural field model proposed by Martinet *et al* in [62] is a modified version of the mean-field model proposed in [78] that seeks to explain the phenomena, origin, and spatiotemporal dynamical properties of seizure propagation and spike-and-wave discharges. Additionally, their work advances the hypothesis that increased diffusion of extracellular potassium concentrations in space influences the interlaced coupling of human seizures (see Supplementary Material for additional details regarding the model). In what follows, we will use the simulated seizure data obtained from the aforementioned model (see details in the Supplementary Material, [62], and table I of [78]) and then consider our closed-loop MPC neurostimulation scheme on the same.

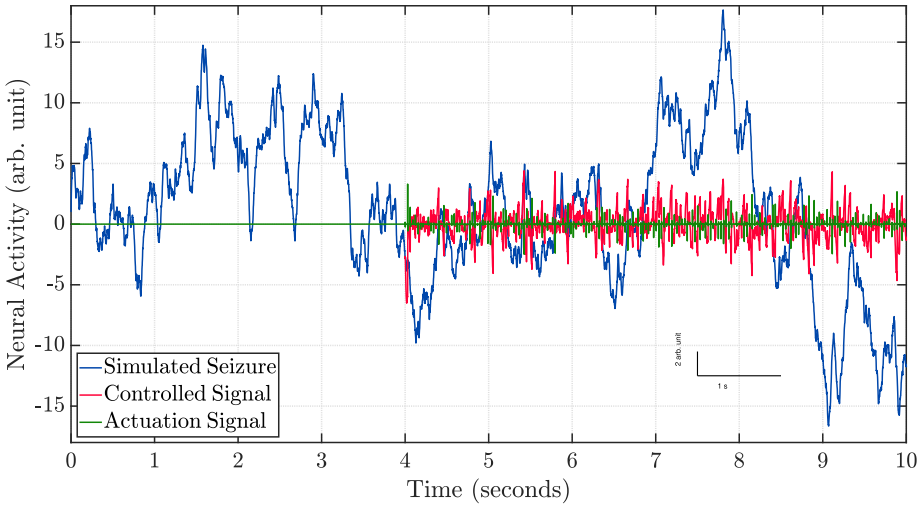

Figure 6. Results of the proposed FOS-MPC closed-loop neurostimulation strategy on an iEEG seizure simulated by the Jansen–Rit neural mass model. The simulated iEEG signal with the seizure is depicted in blue, the controlled signal is depicted in red, and the stimulation pulses are shown in green.

3.2.2. System identification with simulated iEEG data from the model

To determine the system parameters A and α in (10), we utilize roughly 2 s of pre-ictal activity captured by the model. Note that here, we will only consider $n = 4$ channels for our proposed approach to mimic the capabilities available in the NeuroPace® RNS® device. Applying the methods in [16] yields the following FOS parameters:

$$A = \begin{bmatrix} 0.2969 & -0.0203 & -0.2922 & 0.0587 \\ 0.2574 & -0.1726 & -0.1905 & 0.1535 \\ 0.5348 & -0.1066 & -0.3471 & -0.0169 \\ 0.4007 & -0.6752 & 0.0044 & 0.3186 \end{bmatrix}, \tag{11}$$

and

$$\alpha = \begin{bmatrix} 0.8114 & 0.8334 & 0.8034 & 0.8413 \end{bmatrix}^{\mathsf{T}}. \tag{12}$$

Additionally, we consider a single control signal u_k that affects all the channels equally, i.e. $B = \begin{bmatrix} 1 & 1 & 1 & 1 \end{bmatrix}^{\mathsf{T}}$ and the matrix of weights $B^w = 0.05 I_4$, with I_4 being the 4×4 identity matrix.

3.2.3. Closed-loop electrical neurostimulation using FOS-MPC

Using our FOS-MPC neurostimulation strategy with $Q_k = I_n$, $R_k = I_{n_u}$, and $c_k = 0_{n_u \times 1}$ (with $n = 4$ and $n_u = 1$), and safety linear constraints of $-100 \leq u_k \leq 100$, we find from figure 7 that our proposed approach successfully suppresses seizure-like activity using a (time-varying) impulse-like stimulation scheme. In this case, we use a ($p = 10$)-step (20 ms) predictive model approximation of the FOS plant (see Supplementary Material), with a ($P = 10$)-step (20 ms) prediction horizon, and ($M = 8$)-step (16 ms) control horizon. Here too, the actuation signal u_k kicks in at about the 4 s mark.

3.3. Epileptic seizure simulated by the Epileptor, a phenomenological model of seizures by Jirsa *et al* [63]

Next, we investigate the performance of our proposed approach on the Epileptor model [63], which is a phenomenological model able to accurately reproduce the dynamics of a wide variety of human epileptic seizures recorded with iEEG electrodes.

3.3.1. Brief description of the model

The Epileptor is a mathematical model proposed by Jirsa *et al* in [63] and is based on analyzing experimental readings of iEEG seizure discharges in various human and animal subjects. At its core, the model consists of six coupled ordinary differential equations in three time scales that are successfully able to model bistable dynamics between alternating fast discharges and inter-ictal activity, spike-and-wave events (SWEs), and the evolution of the neural populations through the phenomena of seizure onset and offset—see Supplementary Material for a description of the Epileptor model. In what follows, we will use the simulated seizure data obtained from the Epileptor model and implement our closed-loop MPC neuromodulation scheme on it.

3.3.2. System identification and parameter estimation

To determine the parameters A and α that model both spatial coupling and fractional coefficients, respectively, that craft the evolution of the state dynamics in (10), we use the method proposed in [16] Here, like the Jansen–Rit model, the system is SISO, and hence A and α are scalars. The parameters obtained are $A = -0.0051$ and $\alpha = 1.0614$. Furthermore, we assume that $B = 1$ and $B^w = 0.25$.

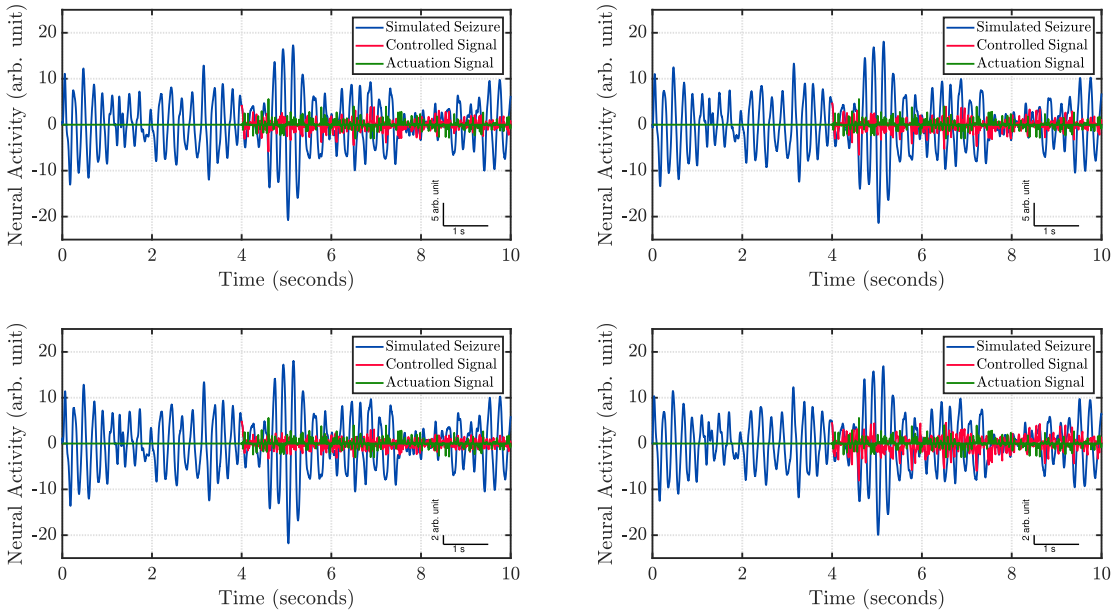

Figure 7. Results of the proposed FOS-MPC closed-loop neurostimulation strategy on an iEEG seizure simulated by the traveling wave dynamics model proposed in [62]. The simulated iEEG signal with the seizure is depicted in blue, the controlled signal is depicted in red, and the stimulation pulses are shown in green.

3.3.3. Closed-Loop electrical neurostimulation using FOS-MPC

We implement our FOS-MPC neurostimulation strategy with $Q_k = I_n$, $R_k = I_{n_u}$, and $c_k = 0_{n_u \times 1}$ (with $n = n_u = 1$) and safety linear constraints of $-50 \leq u_k \leq 50$. In this case, our predictive model was based on a $(p = 20)$–step predictive model approximation of the FOS plant, with a $(P = 20)$-step prediction horizon and $(M = 10)$-step control horizon—see Supplementary Material. The results are presented in figure 8, which provide evidence that the proposed stimulation strategy allows us to achieve amplitude suppression for a seizure simulated by the Epileptor model with standard parameter values.

3.4. Seizure suppression on real seizure data collected from subjects suffering from epilepsy

3.4.1. Overview of our proposed approach

Lastly, we will adopt a data-driven approach, where the underlying model is assumed to be a fractional-order system, on which a FOS-MPC will be considered. Specifically, we test our FOS-MPC strategy under the assumption that the underlying model is fractional in nature, and, as a consequence, captures the evolution of real epileptic seizure data collected from three subjects at the Penn Center for Neuroengineering and Therapeutics, University of Pennsylvania, with four channels depicting the seizure onset. Notice that the sACF of the seizure time series for the first subject in figure 5 further suggests the dependence of the current system states on several past states for time series data of epileptic seizures collected from subjects suffering from the disease.

3.4.2. System identification and parameter estimation

We utilize roughly a second of ictal activity in order to determine the system parameters A and α in (10) using the method proposed in [16]. Here too, we consider $n = 4$ channels. The heatmaps of the values of A and α obtained by performing system identification on the seizure time series data of the three subjects are depicted in figures 9 and 10, respectively. We also consider a single control signal u_k with the matrix $B = \begin{bmatrix} 1 & 0 & 0 & 0 \end{bmatrix}^{\mathsf{T}}$ for subjects 1 and 2 and $B = \begin{bmatrix} 1 & 1 & 1 & 1 \end{bmatrix}^{\mathsf{T}}$ for subject 3. The matrix of weights B^w is assumed to be $B^w = 0.2I_4$, where I_4 is the 4×4 identity matrix.

3.4.3. Closed-loop electrical neurostimulation using FOS-MPC

Next, we use our proposed FOS-MPC neurostimulation strategy with $Q_k = I_n, R_k = I_{n_u}$, and $c_k = 0_{n_u \times 1}$ (with $n = 4$ and $n_u = 1$) and safety linear constraints of $-1000 \leq u_k \leq 1000$ for all the subjects. We use a $(p = 10)$–step (approximately 19.53 ms) predictive model approximation of the FOS plant (see Supplementary Material), with a $(P = 100)$-step (approximately 195.31 ms) prediction horizon and $(M = 80)$-step (approximately 156.25 ms) control horizon for all the simulations. In all of the cases that we consider, the actuation signal u_k is activated 4 s into the start of the simulation. From the figures 11 to 13 we find that we are successfully able to perform amplitude (i.e. seizure) suppression for all the subjects using our proposed approach. We refer the reader to the Supplementary Material for additional results of our scheme on the first subject when the actuation is done in the pre-ictal and post-ictal zone of the seizure depicted

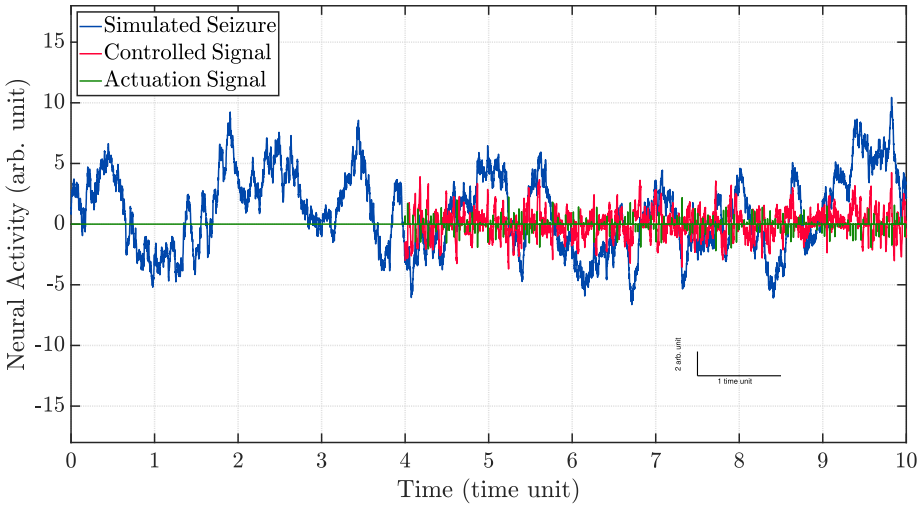

Figure 8. Results of the proposed FOS-MPC closed-loop neurostimulation strategy on an iEEG seizure simulated by the Epileptor model. The simulated iEEG signal with the seizure is depicted in blue, the controlled signal is depicted in red, and the stimulation pulses are shown in green.

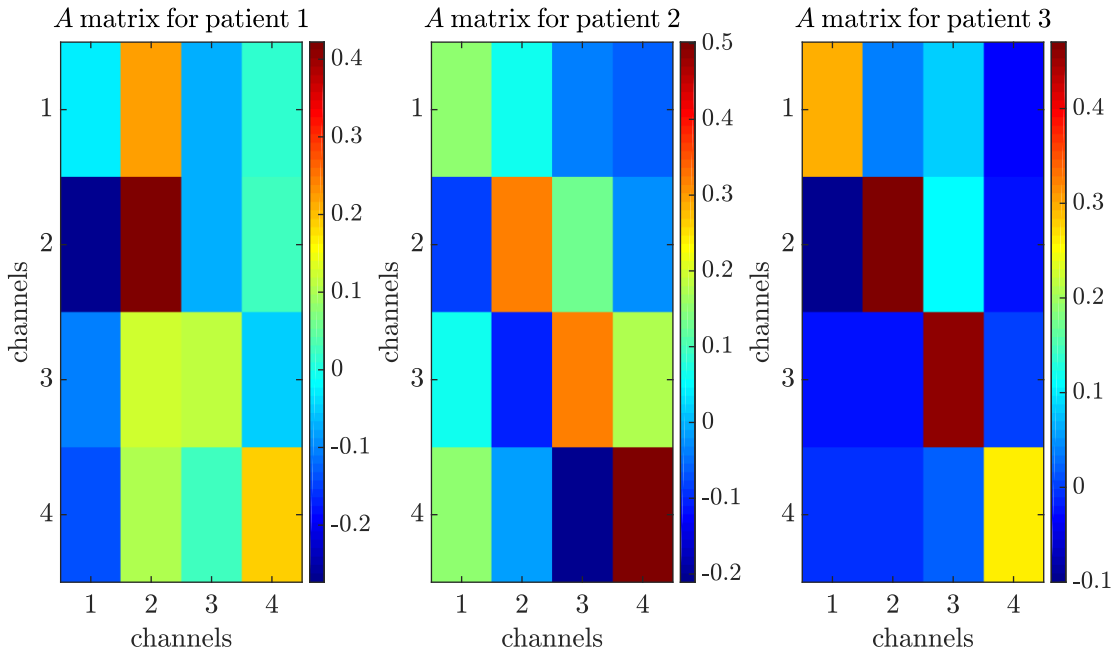

Figure 9. Heatmaps of the *A* matrix for the three subjects considered in our neuromodulation scheme.

in figure 1. This is done so as to provide further evidence that a timely injection of the disruptive stimulus is key, which drives home the need of a closed-loop framework. We also provide results of our scheme for the second subject for varying values of the *B* matrix encapsulating dedicated channel stimulation.

4. Discussion

We presented a methodological framework toward real-time feedback control with constraints for neurophysiological systems. Specifically, we pedagogically introduced a MPC approach when the neurophysiological process can be modeled by a FOS. In doing so, we focused on neurostimulators for epilepsy, and using systems with seizure-like characteristics, we showed that the stimulation strategies obtained by the proposed framework enabled us to mitigate the epileptic seizures. Although we have focused mainly on neurostimulation for epilepsy, we believe that the proposed framework can be readily applied to other forms of neurostimulation with an adequate change in the optimization problem (i.e. in the objective function and constraints).

4.1. Methodological considerations

Unfortunately, there are no widely accepted models for brain dynamics in either healthy or disease

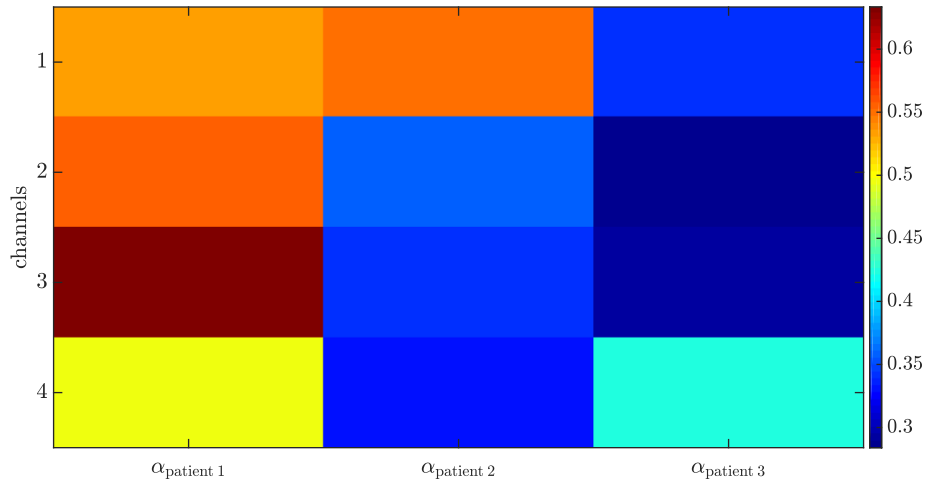

Figure 10. Heatmaps of the fractional-order coefficients α for the three subjects considered in our neuromodulation scheme.

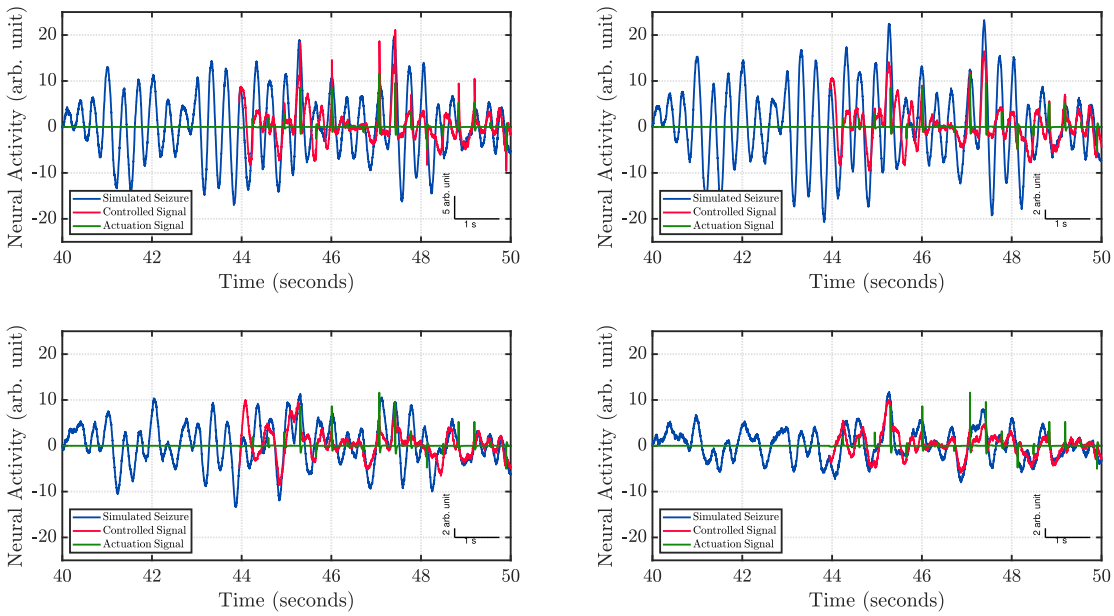

Figure 11. Results of the proposed FOS-MPC closed-loop neurostimulation strategy on iEEG seizure data collected from the first subject with epilepsy during the ictal period. The simulated iEEG signal with the seizure is depicted in blue, the controlled signal is depicted in red, and the stimulation pulses are shown in green.

regimes. As a consequence, we can only argue that fractional-order dynamics has been observed to hold at the level of the neuron [56] and ensembles of neurons as characterized by iEEG technology [10, 13, 15–17].

Furthermore, as suggested by our simulations, some of the adopted models (the Jansen–Rit model [61], the spatiotemporal model of Martinet *et al* [62], and the Epileptor model [63]) exhibit properties that are well captured by FOSs as depicted in figures 2, 3, and 4, as well as in real data (see figure 5) that aligns with previous findings [54, 55]. We can further argue that the behavior captured by the aforementioned technology is local [50]. Subsequently, the local interactions of the electrical stimuli deployed will be immediate, despite the stimulus propagation potentially being anisotropic, which is captured in the proposed model. That said, the best-known models for the analysis of iEEG activity in both healthy and disease regimes are cortical column-like [61, 79], which sometimes fail to incorporate external stimuli as anything other than a persistent noisy stimulus to account for the observed random fluctuations in the data, possibly due to local interactions of the neurological tissue. This is a situation that we have also considered in the simulations conducted in the Simulation Results section.

There are also two key challenges when dealing with noisy data and the proposed FOSs: (*i*) system identification, and (*ii*) determining the feedback control parameters toward practical performance. First,

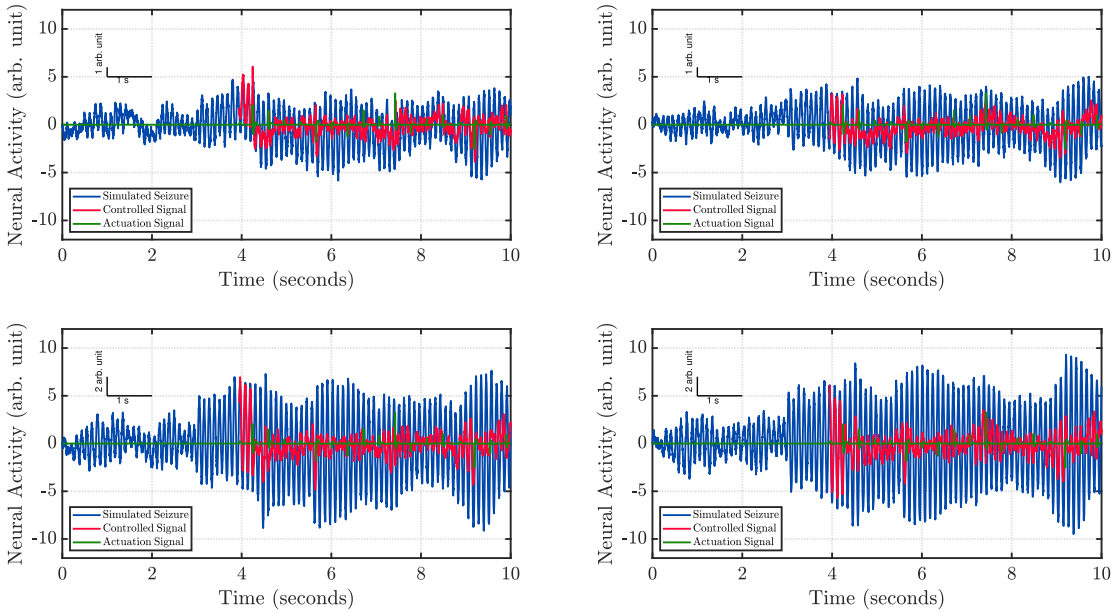

Figure 12. Results of the proposed FOS-MPC closed-loop neurostimulation strategy on iEEG seizure data collected from the second subject with epilepsy during the ictal period. The simulated iEEG signal with the seizure is depicted in blue, the controlled signal is depicted in red, and the stimulation pulses are shown in green.

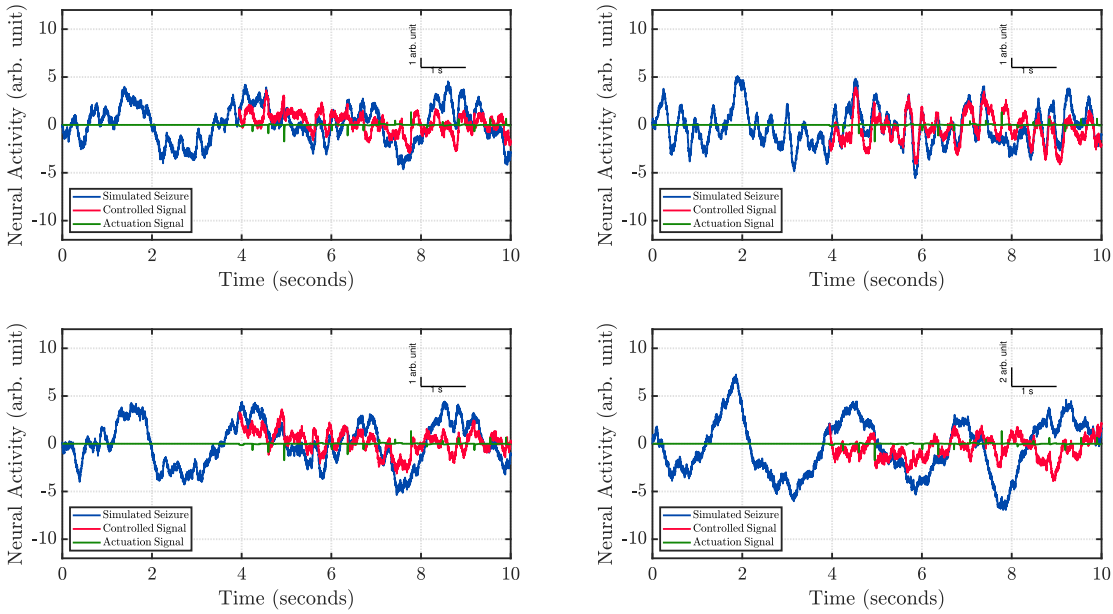

Figure 13. Results of the proposed FOS-MPC closed-loop neurostimulation strategy on iEEG seizure data collected from the third subject with epilepsy during the ictal period. The simulated iEEG signal with the seizure is depicted in blue, the controlled signal is depicted in red, and the stimulation pulses are shown in green.

determining the fractional-order coefficients are known to be sensitive to noise, which consequently will preclude the determination of the coupling state matrix, as spatial and temporal components can be surrogate to each other. In other words, for data that is not justified by the fractional-order coefficients that capture the long-term behavior in time, some system identification method will be used to determine the coupling state matrix to try to account for some of the additional error [80], thus inevitably introducing some bias. Ultimately, despite the existence of methods that try to account for most of the noise while trying to guarantee the FOS to be stationary [9, 16], and considering the highly dynamic nature of brain activity, it becomes imperative in practice to re-identify the system in a timely fashion. This allows models based on fractional-ordered systems to be accommodated within the MPC framework proposed, purposefully introduced in this paper for time-varying systems for that future objective. Nonetheless, we

would also like to mention here that typically, patients with stereotypical and well-localized seizures are the ones that are generally considered to be good candidates for neurostimulation device implants. This implies that off-line calibration of parameters is also an alternative for system identification given we know how the system behaves at seizure onset [81].

4.2. Computational implementation remarks

Any control scheme that requires computationally demanding large-scale optimization methods to be involved, will, in turn, require some form of approximation in order to increase computational efficiency and to enable true real-time control of the system (see Supplementary Material). As such, it is imperative to understand the trade-offs in computational performance involved when using such approximations, which naturally depend from system to system.

The actual dynamics of the brain are highly nonlinear and time-varying. For this reason, it is crucial to re-identify the fractional-order parameters in our predictive model in a real-life implementation of our proposed strategy. Furthermore, considering recent advances regarding MPC implementations on fast-sampled systems [65], we are confident that our strategy is suitable to be programmed into low-powered and low-memory implantable devices similar to the RNS® system. For example, when we are working with the data derived from the first subject, we executed our algorithm in Matlab R2018a running on an x64-based PC with an Intel® Core™ i7-7500U CPU at 2.70 GHz and 16 GB of RAM. The mean running time of the script averaged over 100 runs for each sampled data point was 3.93 ms. With further optimization of our code, we believe that a translation to a lower-level language such as C would lead to a rule-of-thumb 10× improvement in speed. Subsequently, further translating the latter into hardware can give us another possible 2× speed improvement. Furthermore, the recent development in the technology of neurostimulators such as Medtronic's Activa™ RC+S stimulator allows for a cloud-based real-time platform for seizure detection and neurostimulation [82]. In this way, we are not limited by the actual computational power of the neurostimulation device.

Lastly, it should also be noted that in the proposed FOS-MPC stimulation strategy, there are still some design parameters that need to be manually calibrated, such as the prediction horizon P, the control horizon M, the memory horizon p, and the input energy penalization weight $\varepsilon > 0$. Notwithstanding, there is a considerable theoretical foundation dedicated to studying the design of MPC algorithms that achieve stability, robustness, and other performance guarantees [65, 83–85]. This body of results may be used to guide and systematize the parameter calibration stage under a sound and justifiable basis.

4.3. Implications for real-time brain-responsive neurostimulation

Brain-responsive electrical neurostimulation (i.e. closed-loop control electrical stimulation) is key to addressing variations in brain signals that are associated with abnormal behavior. Nonetheless, without the capability of assessing the evolution of the system's dynamics, we will be limited to reactive neurostimulation, i.e. to respond to the last observed state and as a consequence, we will not be able to anticipate the impact of an electric stimulation strategy in the evolution of the brain activity. Such a lack of capabilities may lead to a situation where the stimulation strategy may rather amplify or even create abnormal brain activity that the brain would otherwise resolve.

Even if event-triggered open-loop strategies could be effective in regulating brain activity and mitigating the evolution of seizures (or in minimizing their duration), there is no guarantee or evidence that they would be as energy-efficient as true closed-loop strategies. In other words, the neurostimulator will likely be required to actuate (i.e. release electrical stimulus) more often, with a higher amplitude, and for longer periods of time than with closed-loop mechanisms. Ultimately, this will lead to neurostimulation devices that would do a better use of battery resources which would lead to increased duration periods without the need to replace the battery. As a consequence, this would require the patient to take surgery for the replacement of the battery less often, which will improve the patient's quality of life. Furthermore, the more frequent and unnecessarily extended periods of electrical stimulation may cause additional discomfort that may similarly deteriorate the patient's quality of life [67].

It is also instructive here to note that in closed-loop neuromodulation systems that provide responsive therapies to neurodegenerative disorders, the stimulus signal can be detected by the sensing equipment, thus causing what are known as *stimulation artifacts* that can obfuscate distinctive attributes of the neural signal that is being modulated. However, a compelling body of work provides us with ways of dynamically removing these artifacts, which leads us to conjecture that our proposed algorithm can also be used in conjunction with the aforementioned techniques [86–89].

4.4. Implications for the understanding of brain activity

Several computational models, statistical evidence, and theories have been put forward as attempts to allow us to understand the brain and its dynamics [90–93]. Nonetheless, the gap between these and *in vitro* or *in vivo* validation is still overwhelming. The proposed framework has the advantage to not only assess the data offline but to also interact with the system to collect further data toward the understanding of the input–output relation. As we interact with the

neural tissue through electric stimulation in a real-life context, we will be able to validate how good the models are and change them in real-time by performing system identification with the new data collected by the proposed implantable neurostimulators.

Ultimately, this will provide the validation of FOSs used, which allow for a compact spatiotemporal representation. Specifically, the fractional-order coefficients will enable us to understand the self-dynamics and non-stationary dependency on the past, which is ultimately due to the underlying neurophysiological process. Therefore, this will provide further evidence or new insights into current self-organization theories [7, 94–96]. On the other hand, the dynamic coupling will enable us to understand the spatial dependency on different regions, dynamics, and their change upon an electrical discharge. In particular, it will enable us to easily track the evolution of the electrical stimulus deployed in a heterogeneous and anisotropic environment.

5. Summary and future outlook

Advances in computational processing power made in the last 10–20 years have made the prospects of turning into reality technology that was theoretically devised and previously impossible to implement in real-life. MPC and FOS-based technologies both fall under this category and have thus been significantly overlooked in the industry. However, both of these are growing in popularity amongst certain research communities, and some predict a considerably more widespread impact than originally thought.

The present work lays down a framework and a road-map toward real-time feedback electrical neurostimulation for epilepsy, as a concrete attempt to bring into the biomedical science and engineering community a new tool, in the hopes that it might positively impact society. Furthermore, it aims to pinpoint some limitations and drawbacks of current event-trigged open-loop stimulation strategies (i.e. they can be inefficient or even cause seizure-like activity). As a consequence, it serves as a call for action from neurophysiologists and engineers that work with neurostimulation (as well as DBS) devices, toward validation in *in vitro* and *in vivo* scenarios.

Not with standing, the validation does not suffice to establish a framework since there are several foundational problems that need to be addressed. Specifically, the robustness of the stimulation strategies with respect to the parameters of the models (e.g. the dynamics and the stimuli deployed, as well as the approximations considered to attain real-time stimulation) in devices with low storage, and limited battery and computation capabilities. Toward this goal, only transdisciplinary work between scientists and engineers will lead to success that ultimately will be reflected in the improvement of the quality of life of the patients with neurological disorders (e.g. epilepsy).

5. Acknowledgment

The authors gratefully acknowledge the support by the National Science Foundation under Grant Number CMMI 1936578.

ORCID iDs

Sarthak Chatterjee https://orcid.org/0000-0002-4774-9436
Orlando Romero https://orcid.org/0000-0001-7545-761X
Arian Ashourvan https://orcid.org/0000-0002-1529-7041
Sérgio Pequito https://orcid.org/0000-0002-5143-1543

References

[1] Brodu N, Lotte F and Lécuyer A 2012 Exploring two novel features for EEG-based brain–computer interfaces: multifractal cumulants and predictive complexity *Neurocomputing* **79** 87–94
[2] Suckling J, Wink A M, Bernard F A, Barnes A and Bullmore E 2008 Endogenous multifractal brain dynamics are modulated by age, cholinergic blockade and cognitive performance *J. Neurosci. Methods* **174** 292–300
[3] Ihlen E A and Vereijken B 2010 Interaction-dominant dynamics in human cognition: Beyond $1/f^{\alpha}$ fluctuation *J. Exp. Psychol.: General* **139** 436–463
[4] Ciuciu P, Varoquaux G, Abry P, Sadaghiani S and Kleinschmidt A 2012 Scale-free and multifractal time dynamics of fMRI signals during rest and task *Front. Physiol.* **3** 186
[5] Zorick T and Mandelkern M A 2013 Multifractal detrended fluctuation analysis of human EEG: preliminary investigation and comparison with the wavelet transform modulus maxima technique *PloS One* **8** e68360
[6] Zhang Y, Zhou W and Yuan S 2015 Multifractal analysis and relevance vector machine-based automatic seizure detection in intracranial EEG *Int. J. Neural Syst.* **25** 1550020
[7] Papo D 2014 Functional significance of complex fluctuations in brain activity: from resting state to cognitive neuroscience *Front. Syst. Neurosci.* **8** 112
[8] Tarasov V E 2011 *Fractional Dynamics: Applications of Fractional Calculus to Dynamics of Particles, Fields and Media* (Berlin: Springer Science & Business Media)
[9] Xue Y, Rodriguez S and Bogdan P 2016 A spatio-temporal fractal model for a CPS approach to brain-machine-body interfaces *Proc. of the Design, Automation & Test in Europe (DATE) Conf. & Exhibition* (IEEE) 642–647
[10] Xue Y, Pequito S, Coelho J R, Bogdan P and Pappas G J 2016 Minimum number of sensors to ensure observability of physiological systems: a case study *Proc. of the 54th Annual Allerton Conf. on Communication, Control and Computing* (IEEE) 1181–1188
[11] Xue Y and Bogdan P 2017 Reliable multi-fractal characterization of weighted complex networks: algorithms and implications *Sci. Rep.* **7** 7487
[12] Xue Y and Bogdan P 2017 Constructing compact causal mathematical models for complex dynamics *Proc. of the 8th Int. Conf. on Cyber-Physical Systems* (ACM) 97–107

[13] Pequito S, Bogdan P and Pappas G J 2015 Minimum number of probes for brain dynamics observability *Proc. of the 54th Conf. on Decision and Control* (IEEE) 306–311

[14] Pequito S, Clark A and Pappas G J 2017 Discrete-time fractional-order multiple scenario-based sensor selection *Proc. of the 2017 American Control Conf.* (IEEE) 5488–5493

[15] Tzoumas V, Xue Y, Pequito S, Bogdan P and Pappas G J 2018 Selecting sensors in biological fractional-order systems *IEEE Transactions on Control of Network Systems* **5** 709–721

[16] Gupta G, Pequito S and Bogdan P 2018 Dealing with unknown unknowns: identification and selection of minimal sensing for fractional dynamics with unknown inputs *Proc. of the 2018 American Control Conf.* (IEEE) 2814–2820

[17] Gupta G, Pequito S and Bogdan P 2018 Re-thinking EEG-based non-invasive brain interfaces: modeling and analysis *Proc. of the 9th ACM/IEEE Int. Conf. on Cyber-Physical Systems* (IEEE) 275–286

[18] Dzieliński A and Sierociuk D 2005 Adaptive feedback control of fractional order discrete state-space systems *Proc. of the Int. Conf. on Computational Intelligence for Modeling, Control and Automation and Int. Conf. on Intelligent Agents, Web Technologies and Internet Commerce* (IEEE) (https://doi.org/10.1109/CIMCA.2005.1631363)

[19] Camacho E F and Alba C B 2013 *Model Predictive Control* (Berlin: Springer Science & Business Media)

[20] Mayne D Q, Rawlings J B, Rao C V and Scokaert P O 2000 Constrained model predictive control: Stability and optimality *Automatica* **36** 789–814

[21] Qin S J and Badgwell T A 2003 A survey of industrial model predictive control technology *Control Eng. Pract.* **11** 733–764

[22] Allgöwer F and Zheng A 2012 *Nonlinear Model Predictive Control* (Basel: Birkhäuser) p 26

[23] Garcia C E, Prett D M and Morari M 1989 Model predictive control: theory and practice–a survey *Automatica* **25** 335–348

[24] Morari M and Lee J H 1999 Model predictive control: past, present and future *Comput. Chem. Eng.* **23** 667–682

[25] Schuepbach W M *et al* 2013 Neurostimulation for Parkinson's disease with early motor complications *New Engl. J. Med.* **368** 610–622

[26] Witt K, Granert O, Daniels C, Volkmann J, Falk D, van Eimeren T and Deuschl G 2013 Relation of lead trajectory and electrode position to neuropsychological outcomes of subthalamic neurostimulation in Parkinson's disease: results from a randomized trial *Brain* **136** 2109–2119

[27] Nardone R, Höller Y, Tezzon F, Christova M, Schwenker K, Golaszewski S, Trinka E and Brigo F 2015 Neurostimulation in Alzheimer's disease: from basic research to clinical applications *Neurological Sci.* **36** 689–700

[28] Marangell L, Martinez M, Jurdi R and Zboyan H 2007 Neurostimulation therapies in depression: a review of new modalities *Acta Psychiatrica Scandinavica* **116** 174–181

[29] Bewernick B H *et al* 2010 Nucleus accumbens deep brain stimulation decreases ratings of depression and anxiety in treatment-resistant depression *Biol. Psychiatry* **67** 110–116

[30] Sturm V, Lenartz D, Koulousakis A, Treuer H, Herholz K, Klein J C and Klosterkötter J 2003 The nucleus accumbens: a target for deep-brain stimulation in obsessive-compulsive and anxiety disorders *Journal of Chemical Neuroanatomy* **26** 62–67

[31] Hirtz D, Thurman D, Gwinn-Hardy K, Mohamed M, Chaudhuri A and Zalutsky R 2007 How common are the 'common' neurologic disorders? *Neurology* **68** 326–337

[32] Zack M M and Kobau R 2017 National and state estimates of the numbers of adults and children with active epilepsy-United States, 2015 *Morbidity Mortality Weekly Rep.* **66** 821–825

[33] Fisher R S *et al* 2014 ILAE official report: a practical clinical definition of epilepsy *Epilepsia* **55** 475–482

[34] Ashourvan A *et al* 2017 Parsing spatiotemporal dynamical stability in ECoG during seizure onset, propagation, and termination (arXiv: 1706.08202)

[35] Engel J 2001 A proposed diagnostic scheme for people with epileptic seizures and with epilepsy: report of the ILAE task force on classification and terminology *Epilepsia* **42** 796–803

[36] Perucca E 2006 Clinically relevant drug interactions with antiepileptic drugs *Br. J. Clin. Pharmacol.* **61** 246–255

[37] Binnie C 2000 Vagus nerve stimulation for epilepsy: a review *Seizure* **9** 161–169

[38] Krahl S E 2012 Vagus nerve stimulation for epilepsy: a review of the peripheral mechanisms *Surgical Neurol. Int.* **3** S47-52

[39] Sun F T, Morrell M J and Wharen R E 2008 Responsive cortical stimulation for the treatment of epilepsy *Neurotherapeutics* **5** 68–74

[40] Yu T *et al* 2018 High-frequency stimulation of anterior nucleus of thalamus desynchronizes epileptic network in humans *Brain* **141** 2631–2643

[41] Van Der Vlis T A B, Schijns O E, Schaper F L, Hoogland G, Kubben P, Wagner L, Rouhl R, Temel Y and Ackermans L 2019 Deep brain stimulation of the anterior nucleus of the thalamus for drug-resistant epilepsy *Neurosurgical Rev.* **42** 287–296

[42] Morrell M 2006 Brain stimulation for epilepsy: can scheduled or responsive neurostimulation stop seizures? *Curr. Opinion Neurol.* **19** 164–168

[43] Skarpaas T L and Morrell M J 2009 Intracranial stimulation therapy for epilepsy *Neurotherapeutics* **6** 238–243

[44] Benabid A L 2003 Deep brain stimulation for Parkinson's disease *Curr. Opinion Neurobiol.* **13** 696–706

[45] Thomas G P and Jobst B C 2015 Critical review of the responsive neurostimulator system for epilepsy *Med. Devices* **8** 405–411

[46] Baldassano S N *et al* 2017 Crowdsourcing seizure detection: algorithm development and validation on human implanted device recordings *Brain* **140** 1680–1691

[47] Sun F and Morrell M J 2014 Closed-loop neurostimulation: The clinical experience *Neurotherapeutics* **11** 553–563

[48] Khalil H 2002 *Nonlinear Systems* (Englewood Cliffs, NJ: Pearson Education, Prentice Hall)

[49] Teschl G 2012 *Ordinary Differential Equations and Dynamical Systems* (Providence, RI: American Mathematical Soc.) p 140

[50] Nunez P L and Srinivasan R *et al* 2006 *Electric Fields of the Brain: the Neurophysics of EEG* (Oxford, USA: Oxford University Press)

[51] Hespanha J P 2018 *Linear Systems Theory* (Princeton, New Jersey: Princeton Press)

[52] Chang J, Pigorini A, Seregni F, Massimini M, Nobili L and Veen B D V 2013 Sparse multivariate autoregressive models with exogenous inputs for modeling intracerebral responses to direct electrical stimulation of the human brain *Proc. of the 2013 Asilomar Conf. on Signals, Systems and Computers* (IEEE) 803–807

[53] Grahn P J *et al* 2014 A neurochemical closed-loop controller for deep brain stimulation: toward individualized smart neuromodulation therapies *Front. Neurosci.* **8** 169

[54] Scheffer M *et al* 2009 Early-warning signals for critical transitions *Nature* **461** 53–59

[55] Kramer M A *et al* 2012 Human seizures self-terminate across spatial scales via a critical transition *Proc. Natl Acad. Sci.* 109 21116–121

[56] Lundstrom B N, Higgs M H, Spain W J and Fairhall A L 2008 Fractional differentiation by neocortical pyramidal neurons *Nat. Neurosci.* **11** 1335–1342

[57] Joshi V, Pachori R B and Vijesh A 2014 Classification of ictal and seizure-free EEG signals using fractional linear prediction *Biomed. Signal Process. Control* **9** 1–5

[58] Fei K, Wang W, Yang Q and Tang S 2017 Chaos feature study in fractional Fourier domain for preictal prediction of epileptic seizure *Neurocomputing* **249** 290–298

[59] Liu K, Chen Y and Zhang X 2017 An evaluation of ARFIMA (autoregressive fractional integral moving average) programs *Axioms* **6** 16

[60] Vera-Valdés J E 2020 On long memory origins and forecast horizons *Journal of Forecasting* **39** 811–826
[61] Jansen B H and Rit V G 1995 Electroencephalogram and visual evoked potential generation in a mathematical model of coupled cortical columns *Biol. Cybern.* **73** 357–366
[62] Martinet L-E, Fiddyment G, Madsen J, Eskandar E N, Truccolo W, Eden U T, Cash S and Kramer M A 2017 Human seizures couple across spatial scales through travelling wave dynamics *Nat. Commun.* **8** 1–13
[63] Jirsa V K, Stacey W C, Quilichini P P, Ivanov A I and Bernard C 2014 On the nature of seizure dynamics *Brain* **137** 2210–2230
[64] Rawlings J, Mayne D and Diehl M 2017 *Model Predictive Control: Theory, Computation and Design* (Madison, WI, USA: Nob Hill Publishing)
[65] Zeilinger M N, Jones C N, Raimondo D M and Morari M 2009 Real-time MPC - stability through robust MPC design *Proc. of the 48th Conf. on Decision and Control Held Jointly With the 28th Chinese Control Conf.* (IEEE) 3980–3986
[66] Soltan A, Xia L, Jackson A, Chester G and Degenaar P 2018 Fractional order PID system for suppressing epileptic activities *Proc. of the 2018 IEEE Int. Conf. on Applied System Invention (ICASI)* (IEEE) 338–341
[67] Moratti S and Patterson D 2014 Adverse psychological effects to deep brain stimulation: overturning the question *AJOB Neurosci.* **5** 62–64
[68] Chatterjee S, Romero O and Pequito S 2019 A separation principle for discrete-time fractional-order dynamical systems and its implications to closed-loop neurotechnology *IEEE Control Syst. Lett.* **3** 691–696
[69] Bequette B W 2013 Algorithms for a closed-loop artificial pancreas: the case for model predictive control *J. Diabetes Sci. Technol.* **7** 1632–1643
[70] Jansen B H, Zouridakis G and Brandt M E 1993 A neurophysiologically-based mathematical model of flash visual evoked potentials *Biol. Cybern.* **68** 275–283
[71] Wendling F, Bellanger J-J, Bartolomei F and Chauvel P 2000 Relevance of nonlinear lumped-parameter models in the analysis of depth-EEG epileptic signals *Biol. Cybern.* **83** 367–378
[72] Wendling F, Benquet P, Bartolomei F and Jirsa V 2016 Computational models of epileptiform activity *J. Neurosci. Methods* **260** 233–251
[73] Wang J, Niebur E, Hu J and Li X 2016 Suppressing epileptic activity in a neural mass model using a closed-loop proportional-integral controller *Sci. Rep.* **6** 27344
[74] Xia L, Soltan A, Zhang X, Jackson A, Tessier R and Degenaar P 2019 Closed-loop proportion-derivative control of suppressing seizures in a neural mass model *Proc. of the 2019 IEEE Int. Symp. on Circuits and Systems (ISCAS)* (IEEE) 1–5
[75] Wei W, Wei X, Zuo M, Yu T and Li Y 2019 Seizure control in a neural mass model by an active disturbance rejection approach *Int. J. Adv. Robotic Syst.* **16** 1729881419890152
[76] Wei W, Wei X, Xia P, Zuo M and Shen D 2019 Seizure control by a learning type active disturbance rejection approach *IEEE Access* **7** 164792–164802
[77] Wei W, Wei X and Zuo M 2019 Control of epileptiform waves in a neural mass model *Proc. of the 2019 Chinese Control Conf. (CCC)* (IEEE) 6860–6864
[78] Steyn-Ross M L, Steyn-Ross D A and Sleigh J W 2013 Interacting Turing-Hopf instabilities drive symmetry-breaking transitions in a mean-field model of the cortex: a mechanism for the slow oscillation *Phys. Rev. X* **3** 021005
[79] Grimbert F and Faugeras O 2006 Analysis of Jansen's model of a single cortical column *PhD Dissertation* INRIA
[80] Sierociuk D and Dzieliński A 2006 Fractional Kalman filter algorithm for the states parameters and order of fractional system estimation *Int. J. Appl. Math. Computer Sci.* **16** 129–140
[81] Ashourvan A *et al* 2020 Model-based design for seizure control by stimulation *J. Neural Eng.* **17** 026009
[82] Baldassano S, Zhao X, Brinkmann B, Kremen V, Bernabei J, Cook M, Denison T, Worrell G and Litt B 2019 Cloud computing for seizure detection in implanted neural devices *J. Neural Eng.* **16** 026016
[83] Cheng X and Krogh B H 2001 Stability-constrained model predictive control *IEEE Trans. Autom. Control* **46** 1816–1820
[84] El-Farra N H, Mhaskar P and Christofides P D 2002 Uniting bounded control and MPC for stabilization of constrained linear systems *Automatica* 101–110
[85] Pannek J and Worthmann K 2014 Stability and performance guarantees for model predictive control algorithms without terminal constraints *ZAMM J. Appl. Math. Mech.: Zeitschrift für angewandte Mathematik und Mechanik* **94** 317–330
[86] Keller T and Popovic M R 2001 Real-time stimulation artifact removal in EMG signals for neuroprosthesis control applications *Proc. of the IFESS' 2000th Conf.* (*Cleveland, USA*)
[87] Wagenaar D A and Potter S M 2002 Real-time multi-channel stimulus artifact suppression by local curve fitting *J. Neurosci. Methods* **120** 113–120
[88] Limnuson K, Lu H, Chiel H J and Mohseni P 2013 Real-time stimulus artifact rejection via template subtraction *IEEE Trans. Biomed. Circuits Syst.* **8** 391–400
[89] Zhou A, Johnson B C and Muller R 2018 Toward true closed-loop neuromodulation: artifact-free recording during stimulation *Curr. Opinion Neurobiol.* **50** 119–127
[90] Nunez P L and Silberstein R B 2000 On the relationship of synaptic activity to macroscopic measurements: does co-registration of EEG with fMRI make sense? *Brain Topogr.* **13** 79–96
[91] Brunel N and Wang X-J 2003 What determines the frequency of fast network oscillations with irregular neural discharges? I. Synaptic dynamics and excitation-inhibition balance *J. Neurophysiol.* **90** 415–430
[92] Breakspear M and Jirsa V K 2007 Neuronal dynamics and brain connectivity in *Handbook of Brain Connectivity* (Berlin: Springer) 3–64
[93] Stefanescu R A and Jirsa V K 2011 Reduced representations of heterogeneous mixed neural networks with synaptic coupling *Phys. Rev.* E **83** 026204
[94] Bak P, Tang C and Wiesenfeld K 1987 Self-organized criticality: an explanation of the 1/*f* noise *Phys. Rev. Lett.* **59** 381–384
[95] Fraiman D and Chialvo D R 2012 What kind of noise is brain noise: anomalous scaling behavior of the resting brain activity fluctuations *Front. Physiol.* **3** 307
[96] Solovey G, Miller K J, Ojemann J, Magnasco M O and Cecchi G A 2012 Self-regulated dynamical criticality in human ECoG *Front. Integrative Neurosci.* **6** 44